INTERNATIONAL JOURNAL OF
ENERGY AND ENVIRONMENT

Volume 3, Issue 4, 2012 pp.505-520

Journal homepage: www.IJEE.IEEFoundation.org

Exergoeconomic performance optimization of an endoreversible intercooled regenerative Brayton combined heat and power plant coupled to variable-temperature heat reservoirs

Bo Yang, Lingen Chen, Fengrui Sun

College of Naval Architecture and Power, Naval University of Engineering, Wuhan 430033, P. R. China.

Abstract
An endoreversible intercooled regenerative Brayton combined heat and power (CHP) plant model coupled to variable-temperature heat reservoirs is established. The exergoeconomic performance of the CHP plant is investigated using finite time thermodynamics. The analytical formulae about dimensionless profit rate and exergy efficiency of the CHP plant with the heat resistance losses in the hot-, cold- and consumer-side heat exchangers, the intercooler and the regenerator are deduced. By taking the maximum profit rate as the objective, the heat conductance allocation among the five heat exchangers and the choice of intercooling pressure ratio are optimized by numerical examples, the characteristic of the optimal dimensionless profit rate versus corresponding exergy efficiency is investigated. When the optimization is performed further with respect to the total pressure ratio, a double-maximum profit rate is obtained. The effects of the design parameters on the double-maximum dimensionless profit rate and corresponding exergy efficiency, optimal total pressure ratio and optimal intercooling pressure ratio are analyzed in detail, and it is found that there exist an optimal consumer-side temperature and an optimal thermal capacitance rate matching between the working fluid and the heat reservoir, respectively, corresponding to a thrice-maximum dimensionless profit rate.

Keywords: Finite time thermodynamics; Intercooled regenerative Brayton combined heat and power plant; Exergoeconomic performance; Profit rate; Optimization.

1. Introduction

Combined heat and power (CHP) plants in which heat and power are produced together are now widely used and are more advantageous in terms of energy and exergy efficiencies than plants which produce heat and power separately [1]. It is important to determine the optimal design parameters of the CHP plants. By using classical thermodynamics, Rosen *et al* [2] performed energy and exergy analyses for CHP-based district energy systems and exergy methods are employed to evaluated overall and component efficiencies and to identify and assess thermodynamic losses. Khaliq [3] performed the exergy analysis of a gas turbine trigeneration system for combined production of power, heat and refrigeration and investigated the effects of overall pressure ratio, turbine inlet temperature, and pressure drop on the exergy destruction. Reddy and Butcher [4] investigated the exergetic efficiency performance of a natural gas-fired intercooled reheat gas turbine CHP system and analyzed the effects of interooling,

reheat and total pressure ratio on the performance of the CHP plant. Khaliq and Choudhary [5] evaluated the performance of intercooled reheat regenerative gas turbine CHP plant by using the first law (energetic efficiency) and second law (exergetic efficiency) of thermodynamics and investigated the effects of overall pressure ratio, cycle temperature ratio, pressure losses on the performance of the CHP plant.

Finite-time thermodynamics (FTT) [6-18] is a powerful tool for analyzing and optimizing performance of various thermodynamic cycles and devices. Some authors have performed the performance analysis and optimization for various CHP plants by using finite-time thermodynamics. Bojic [19] investigated the annual worth of an endoreversible Carnot cycle CHP plant with the sole irreversibility of heat resistance. Sahin *et al* [20] performed exergy output rate optimization for an endoreversible Carnot cycle CHP plant and found that the lower the consumer-side temperature, the better the performance. Erdil *et al* [21] optimized the exergetic output rate and exergetic efficiency of an irreversible combined Carnot cycle CHP plant under various design and operating conditions and found that the optimal performance stayed approximately constant with consumer-side temperature. Atmaca *et al* [22] performed the exergetic output rate, energy utilization factor (EUF), artificial thermal efficiency and exergetic efficiency optimization of an irreversible Carnot cycle CHP plant. Ust *et al* [23] provided a new exergetic performance criterion, exergy density, which includes the consideration of the system sizes, and investigated the general and optimal performances of an irreversible Carnot cycle CHP plant.

In industry, Brayton cycle is widely used. some authors are interested in the CHP plants composed of various Brayton cycles. Yilmaz [24] optimized the exergy output rate and exergetic efficiency of an endoreversible simple gas turbine closed-cycle CHP plant, investigated the effects of parameters on exergetic performance and found that the lower the consumer-side temperature, the better the performance. Hao and Zhang [25, 26] optimized the total useful-energy rate (including power output and useful heat rate output) and the exergetic output rate of an endoreversible Joule-Brayton CHP cycle by optimizing the pressure ratio and analyzed the effects of design parameters on the optimal performances. Ust *et al* [27, 28] proposed a new objective function called the exergetic performance coefficient (EPC), optimized an irreversible regenerative gas turbine closed-cycle CHP plant with heat resistance and internal irreversibility [27] and an irreversible Dual cycle CHP plant with heat resistance, heat leakage and internal irreversibility [28], and compared the results with those obtained using the total exergy output as the objective.

Exergoeconomic (or thermoeconomic) analysis and optimization [29, 30] is a relatively new method that combines exergy with conventional concepts from long-run engineering economic optimization to evaluate and optimize the design and performance of energy systems. Salamon and Nitzan [31] combined the endoreversible model with exergoeconomic analysis for endoreversible Carnot heat engine with the only loss of heat resistance. It was termed as finite time exergoeconomic analysis [32-38] to distinguish it from the endoreversible analysis with pure thermodynamic objectives and the exergoeconomic analysis with long-run economic optimization. Furthermore, such a method has been extended to universal endoreversible heat engine [39] and generalized irreversible Carnot heat engine [40] and refrigerator [41]. On the basis of Refs. [32-41], Tao *et al* [42, 43] performed the finite time exergoeconomic performance analysis and optimization for endoreversible simple [42] and regenerative [43] gas turbine closed-cycle CHP plant coupled to constant temperature heat reservoirs by optimizing the heat conductance allocation among the hot-, cold- and consumer-side heat exchangers, the regenerator and the pressure ratio of the compressor. Chen *et al* [44] and Yang *et al* [45] analyzed and optimized the finite time exergoeconomic performance of an endoreversible intercooled regenerative Brayton CHP plant coupled to constant-temperature heat reservoirs.

A thermodynamic model of an endoreversible intercooled regenerative Brayton CHP plant coupled to variable-temperature heat reservoirs was established in Ref. [46]. The performance investigation and parametric analysis were performed by using finite time exergoeconomic analysis. The analytical formulae about dimensionless profit rate and exergy efficiency were deduced, respectively [46]. A further step made in this paper is to optimize the heat conductance allocation among the hot-, cold- and consumer-side heat exchangers, the intercooler and the regenerator, the intercooling pressure ratio and the total pressure ratio by taking the maximum dimensionless profit rate as the objective. Effects of design parameters on the optimal performance are analyzed in detail and the thermal capacitance rate matching between the working fluid and the heat reservoir is discussed.

2. Cycle model

A T-s diagram of CHP plant composed of an endoreversible intercooled regenerative Brayton closed-cycle coupled to variable-temperature heat reservoirs is shown in Figure 1. Process 1-2 and 3-4 are isentropic adiabatic compression processes in the low- and high-pressure compressors, while the process 5-6 is isentropic adiabatic expansion process in the turbine. Process 2-3 is an isobaric intercooling process in the intercooler. Process 4-7 is an isobaric absorbed heat process and process 6-8 is an isobaric evolved heat process in the regenerator. Process 7-5 is an isobaric absorbed heat process in the hot-side heat exchanger and process 9-1 is an isobaric evolved heat process in the cold-side heat exchanger. Process 8-9 is an isobaric evolved heat process in the customer-side heat exchanger.

Assuming that the working fluid used in the cycle is an ideal gas with constant thermal capacity rate (mass flow rate and specific heat product) C_{wf}. The hot-side heat reservoir is considered to have a thermal capacity rate C_H and the inlet and the outlet temperatures of the heating fluid are T_{Hin} and T_{Hout}, respectively. The cold-side heat reservoir is considered to have a thermal capacity rate C_L and the inlet and the outlet temperatures of the cooling fluid are T_{Lin} and T_{Lout}, respectively. The cooling fluid in the intercooler is considered to have a thermal capacity rate C_I and the inlet and the outlet temperatures of the cooling fluid are T_{Iin} and T_{Iout}, respectively. The consumer-side temperature is T_K. The heat exchangers between the working fluid and the heat reservoir, the regenerator and the intercooler are counter-flow and the heat conductances (heat transfer surface area and heat transfer coefficient product) of the hot-, cold- and consumer-side heat exchangers, the intercooler and the regenerator are U_H, U_L, U_K, U_I, U_R respectively. According to the heat transfer processes, the properties of the heat reservoirs and working fluid, and the theory of heat exchangers, the rate (Q_H) of heat transfer from heat source to the working fluid, the rate (Q_L) of heat transfer from the working fluid to the heat sink, the rate (Q_K) of heat transfer from the working fluid to the heat consuming device, the rate (Q_I) of heat exchanged in the intercooler, and the rate (Q_R) of heat regenerated in the regenerator are, respectively, given by:

$$Q_H = U_H \frac{(T_{Hin}-T_5)-(T_{Hout}-T_7)}{\ln\left[(T_{Hin}-T_5)/(T_{Hout}-T_7)\right]} = C_H(T_{Hin}-T_{Hout}) = C_{wf}(T_5-T_7) = C_{H\min}E_{H1}(T_{Hin}-T_7) \tag{1}$$

$$Q_L = U_L \frac{(T_9-T_{Lout})-(T_1-T_{Lin})}{\ln\left[(T_9-T_{Lout})/(T_1-T_{Lin})\right]} = C_L(T_{Lout}-T_{Lin}) = C_{wf}(T_9-T_1) = C_{L\min}E_{L1}(T_9-T_{Lin}) \tag{2}$$

$$Q_K = U_K \frac{T_8-T_9}{\ln[(T_8-T_K)/(T_9-T_K)]} = C_{wf}(T_8-T_9) = C_{wf}E_K(T_8-T_K) \tag{3}$$

$$Q_I = U_I \frac{(T_2-T_{Iout})-(T_3-T_{Iin})}{\ln\left[(T_2-T_{Iout})/(T_3-T_{Iin})\right]} = C_I(T_{Iout}-T_{Iin}) = C_{wf}(T_2-T_3) = C_{\mathrm{Im}in}E_{I1}(T_2-T_{Iin}) \tag{4}$$

$$Q_R = C_{wf}(T_7-T_4) = C_{wf}(T_6-T_8) = C_{wf}E_R(T_6-T_4) \tag{5}$$

where E_{H1}, E_{L1}, E_K, E_{I1} and E_R are the effectivenesses of the hot-, cold-, consumer-side heat exchangers, the intercooler and the regenerator, respectively, and are defined as:

$$E_{H1} = \frac{1-\exp\left[-N_{H1}(1-C_{H\min}/C_{H\max})\right]}{1-(C_{H\min}/C_{H\max})\exp\left[-N_{H1}(1-C_{H\min}/C_{H\max})\right]} \tag{6}$$

$$E_{L1} = \frac{1-\exp\left[-N_{L1}(1-C_{L\min}/C_{L\max})\right]}{1-(C_{L\min}/C_{L\max})\exp\left[-N_{L1}(1-C_{L\min}/C_{L\max})\right]} \tag{7}$$

$$E_K = 1-\exp(-N_K) \tag{8}$$

$$E_{I1}=\frac{1-\exp\left[-N_{I1}(1-C_{\mathrm{Im}in}/C_{\mathrm{Im}ax})\right]}{1-(C_{\mathrm{Im}in}/C_{\mathrm{Im}ax})\exp\left[-N_{I1}(1-C_{\mathrm{Im}in}/C_{\mathrm{Im}ax})\right]} \tag{9}$$

$$E_R=N_R/(N_R+1) \tag{10}$$

where $C_{H\min}$ and $C_{H\max}$ are the smaller and the larger of the two capacitance rates C_H and C_{wf}, $C_{L\min}$ and $C_{L\max}$ are the smaller and the larger of the two capacitance rates C_L and C_{wf}, $C_{\mathrm{Im}in}$ and $C_{\mathrm{Im}ax}$ are the smaller and the larger of the two capacitance rates C_I and C_{wf}. N_{H1}, N_{L1}, N_K, N_{I1} and N_R are the numbers of heat transfer units of the hot-side, cold-side, consumer-side heat exchangers, the intercooler and the regenerator, respectively, and are defined as:

$$\begin{aligned}&N_{H1}=U_H/C_{H\min},\ N_{L1}=U_L/C_{L\min},\ N_K=U_K/C_{wf},\ N_{I1}=U_I/C_{\mathrm{Im}in},\ N_R=U_R/C_{wf}\\&C_{H\min}=\min\{C_H,C_{wf}\},\ C_{H\max}=\max\{C_H,C_{wf}\},\ C_{L\min}=\min\{C_L,C_{wf}\}\\&C_{L\max}=\max\{C_L,C_{wf}\},\ C_{\mathrm{Im}in}=\min\{C_I,C_{wf}\},\ C_{\mathrm{Im}ax}=\max\{C_I,C_{wf}\}\end{aligned} \tag{11}$$

Defining the working fluid isentropic temperature ratios x and y for the low-pressure compressor and the total compression process, i.e. $x=T_2/T_1$ and $y=T_5/T_6$. According to the properties of endoreversible process, one has:

$$x=\pi_1^{(k-1)/k},\ \ y=\pi^{(k-1)/k},\ \ T_4=T_3yx^{-1} \tag{12}$$

where π_1 is the intercooling pressure ratio which satisfies $\pi_1\geq 1$, π is the total pressure ratio which satisfies $\pi\geq\pi_1$, and k is the specific heat ratio of the working fluid.

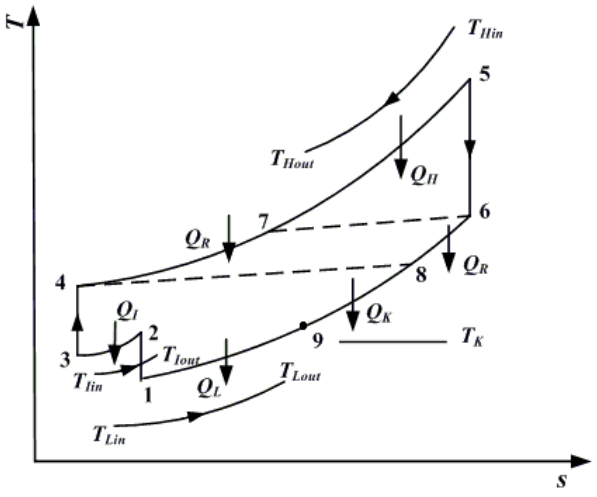

Figure 1. *T*-*s* diagram for the cycle process

3. The profit rate and exergy efficiency analytical formulae [46]

Assuming the environment temperature is T_0, the total rate of exergy input of the CHP plant is:

$$\begin{aligned}e_H&=\int_{T_{Hout}}^{T_{Hin}}(1-T_0/T)C_H\,dT-\int_{T_{Lin}}^{T_{Lout}}(1-T_0/T)C_L\,dT-\int_{T_{Iin}}^{T_{Iout}}(1-T_0/T)C_I\,dT\\&=Q_H-Q_L-Q_I-T_0\left[C_H\ln(T_{Hin}/T_{Hout})-C_L\ln(T_{Lout}/T_{Lin})-C_I\ln(T_{Iout}/T_{Iin})\right]\end{aligned} \tag{13}$$

According to the first law of thermodynamics, the power output (the exergy output rate of power) of the CHP plant is:

$$P = Q_H - Q_L - Q_I - Q_K \tag{14}$$

The entropy generation rate of the CHP plant is:

$$\sigma = C_L \ln(T_{Lout}/T_{Lin}) + C_I \ln(T_{Iout}/T_{Iin}) + Q_K/T_K - C_H \ln(T_{Hin}/T_{Hout}) \tag{15}$$

From the exergy conservation principle for the CHP plant, one has:

$$e_H = P + e_K + T_0\sigma \tag{16}$$

where e_K is thermal exergy output rate, i.e. the exergy output rate of process heat, $T_0\sigma$ is the exergy loss rate.
Combining equations (13)-(16), the thermal exergy output rate e_K can be written as:

$$e_K = Q_K(1 - T_0/T_K) \tag{17}$$

Assuming that the prices of exergy input rate, power output and thermal exergy output rate be φ_H, φ_P and φ_K, respectively, the profit rate of CHP plant is:

$$\Pi = \varphi_P P + \varphi_K e_K - \varphi_H e_H \tag{18}$$

When $\varphi_P = \varphi_K = \varphi_H$, equation (18) becomes:

$$\Pi = \varphi_P(P + e_K - e_H) = -\varphi_P T_0 \sigma \tag{19}$$

The maximum profit rate objective is equivalent to a minimum entropy generation rate objective in this case.
When $\varphi_P = \varphi_K$ and $\varphi_H/\varphi_P \to 0$, equation (18) becomes:

$$\Pi = \varphi_P(P + e_K) \tag{20}$$

The maximum profit rate objective is equivalent to a maximum total exergy output rate objective in this case.
Combining equations (1)-(5) with (12)-(17) yields the inlet temperature of the low-pressure compressor:

$$T_1 = \frac{\begin{array}{l} 2yc_2c_4T_{Iin}E_{I1}C_{\mathrm{Im}in}[c_3(c_1-1) + yE_RC_{wf}] + x[2C_{wf}(c_4T_K + T_{Lin}E_{L1}C_{L\min}) \\ (yC_{wf} - c_3E_R) + 2c_2c_4T_KC_{wf}(c_3 - yC_{wf}) + c_1c_2c_4C_{wf}(T_{Hin}E_{H1}C_{H\min} - c_3T_K)] \end{array}}{2x\{{C_{wf}}^2(yC_{wf} - c_3E_R) + yc_2c_4c_5[c_3(1-c_1) - yE_RC_{wf}]\}} \tag{21}$$

where

$$c_1 = 2(1-E_R),\ c_2 = 1 - E_K,\ c_3 = C_{wf} - C_{H\min}E_{H1},\ c_4 = C_{wf} - C_{L\min}E_{L1},\ c_5 = C_{wf} - C_{\mathrm{Im}in}E_{I1} \tag{22}$$

The power output is:

$$P = \frac{\begin{array}{l} C_{H\min}E_{H1}[xc_2c_4C_{wf}T_{Hin}(1-E_R) - xyC_{wf}(T_1C_{wf} - C_{L\min}E_{L1}T_{Lin} - c_4E_KT_K) + c_2c_4E_Ry^2 \\ (xc_5T_1 + C_{I\min}E_{I1}T_{Iin})] - xc_3(1-E_R)[c_2C_{wf}C_{L\min}E_{L1}(T_1 - T_{Lin}) + c_2c_4C_{I\min}E_{I1}(xT_1 - \\ T_{Iin}) + C_{wf}E_K(T_1C_{wf} - C_{L\min}E_{L1}T_{Lin} - c_4T_K)] \end{array}}{xc_2c_3c_4(1-E_R)} \tag{23}$$

The thermal exergy output rate is:

$$e_K = \frac{C_{wf}E_K(T_K - T_0)(T_1C_{wf} - C_{L\min}E_{L1}T_{Lin} - c_4T_K)}{c_2c_4T_K} \tag{24}$$

Defining price ratios $a = \varphi_P/\varphi_H$, $b = \varphi_K/\varphi_H$, Π can be nondimensionalized by using $\varphi_H C_{wf} T_0$:

$$\overline{\Pi} = \frac{\varphi_P P + \varphi_K e_K - \varphi_H e_H}{\varphi_H C_{wf} T_0} = \frac{(a-1)P + (b-1)e_K - T_0\sigma}{C_{wf}T_0} \tag{25}$$

The exergy efficiency (η_{ex}) is defined as the ratio of total exergy output rate to total exergy input rate:

$$\eta_{ex} = \frac{P + e_K}{e_H} = \frac{P + e_K}{P + e_K + T_0\sigma} \tag{26}$$

where

$$\begin{aligned}\sigma = {} & C_H \ln\{1 - C_{H\min}E_{H1}[xc_2c_4C_{wf}T_{Hin}(1-E_R) - xyC_{wf}(T_1C_{wf} - C_{L\min}E_{L1}T_{Lin} - c_4E_KT_K) + \\ & c_2c_4E_Ry^2(xc_5T_1 + C_{I\min}E_{I1}T_{Iin})]/[xc_2c_3c_4C_HT_{Hin}(1-E_R)]\} + C_L\ln[1 + C_{wf}C_{L\min}E_{L1} \\ & (T_1 - T_{Lin})/(c_4C_LT_{Lin})] + C_I\ln[1 + C_{I\min}E_{I1}(xT_1 - T_{Iin})/(C_IT_{Iin})] + C_{wf}E_K(T_1C_{wf} - \\ & C_{L\min}E_{L1}T_{Lin} - c_4T_K)/(c_2c_4T_K)\end{aligned} \tag{27}$$

4. Finite time exergoeconomic performance optimization

According to equations (25) and (26), the dimensionless profit rate $\overline{\Pi}$ and exergy efficiency η_{ex} of the endoreversible intercooled regenerative Brayton CHP plant coupled to variable- temperature heat reservoirs are the functions of the intercooling pressure ratio (π_1), the total pressure ratio (π) and the five heat conductances (U_H, U_L, U_K, U_I, U_R) when the other boundary condition parameters (a, b, T_{Hin}, T_{Lin}, T_{Iin}, T_K, C_H, C_L, C_I, C_{wf}) are fixed. In practical design, π_1, π, U_H, U_L, U_K, U_I and U_R are changeable and the cost per unit of heat conductance may be different for each heat exchanger because different materials may be used. To simplify the problem, the constraint on total heat exchanger inventory is used for the performance optimization of intercooled regenerated Brayton cycles as Refs. [47-49] by taking power, efficiency and power density as the objectives.

Assuming that the total heat exchanger inventory ($U_T = U_H + U_L + U_K + U_I + U_R$) is fixed, a group of heat conductance allocations are defined as:

$$u_h = U_H/U_T, u_l = U_L/U_T, u_k = U_K/U_T, u_i = U_I/U_T, u_r = U_R/U_T \tag{28}$$

Additionally, one has the constraints:

$$0 < u_h < 1, 0 < u_l < 1, 0 < u_k < 1, 0 < u_i < 1, 0 < u_r < 1, u_h + u_l + u_k + u_i + u_r = 1 \tag{29}$$

For the fixed π, π_1 and U_T, the optimization can be performed by searching the optimal heat conductance allocations ($(u_h)_{\overline{\Pi}_{opt}}$, $(u_l)_{\overline{\Pi}_{opt}}$, $(u_k)_{\overline{\Pi}_{opt}}$, $(u_i)_{\overline{\Pi}_{opt}}$, $(u_r)_{\overline{\Pi}_{opt}}$) which lead to the optimal dimensionless profit rate ($\overline{\Pi}_{opt}$), and one can always obtain $(u_r)_{\overline{\Pi}_{opt}} = 0$. The reason is that regeneration makes the optimal dimensionless profit rate decrease.

When u_r, π and U_T is fixed, the optimization can be performed by searching the other four optimal heat conductance allocations ($(u_h)_{\overline{\Pi}_{\max}}$, $(u_l)_{\overline{\Pi}_{\max}}$, $(u_k)_{\overline{\Pi}_{\max}}$, $(u_i)_{\overline{\Pi}_{\max}}$) and the optimal intercooling pressure ratio ($(\pi_1)_{\overline{\Pi}_{\max}}$) which lead to the maximum dimensionless profit rate ($\overline{\Pi}_{\max}$). If π is changeable, the double-maximum dimensionless profit rate ($\overline{\Pi}_{\max,2}$) and the corresponding exergy efficiency ($(\eta_{ex})_{\overline{\Pi}_{\max,2}}$), optimal total pressure ratio ($\pi_{\overline{\Pi}_{\max,2}}$) and optimal intercooling pressure ratio ($(\pi_1)_{\overline{\Pi}_{\max,2}}$) can be obtained.

To search the optimal values of u_h, u_l, u_k, u_i, π_1 and π, numerical calculations are provided by using the optimization toolbox of Matlab 7.1. In the calculations, four temperature ratios are defined: $\tau_1 = T_{Hin}/T_0$, $\tau_2 = T_{Lin}/T_0$, $\tau_3 = T_{Iin}/T_0$ and $\tau_4 = T_K/T_0$, and $U_T = 10kW/K$, $u_r = 0.1$, $k = 1.4$, $C_{wf} = 1.0kW/K$, $C_H = C_L = C_I = 1.2kW/K$, $\tau_1 = 5$, $\tau_2 = \tau_3 = 1$ and $\tau_4 = 1.2$ are set. According to analysis in Ref. [50], $a = 10$ and $b = 6$ are set.

4.1 The optimal dimensionless profit rate

Assuming that $\pi = 15$ $(1 \le \pi_1 \le \pi)$. Figure 2 shows the characteristic of the optimal dimensionless profit rate ($\overline{\Pi}_{opt}$) versus π_1 for different τ_1. It can be seen that there exists an optimal intercooling pressure ratio ($(\pi_1)_{\overline{\Pi}_{\max}}$) which make $\overline{\Pi}_{opt}$ reach the maximum dimensionless profit rate ($\overline{\Pi}_{\max}$). That is, there exists a sole group of optimal heat conductance allocations ($(u_h)_{\overline{\Pi}_{\max}}$, $(u_l)_{\overline{\Pi}_{\max}}$, $(u_k)_{\overline{\Pi}_{\max}}$, $(u_i)_{\overline{\Pi}_{\max}}$) and an optimal intercooling pressure ratio ($(\pi_1)_{\overline{\Pi}_{\max}}$) which lead to the maximum dimensionless profit rate ($\overline{\Pi}_{\max}$). $\overline{\Pi}_{opt}$ increases with the increase of τ_1. The calculation illustrates that when π_1 increases to a certain value, one has $(u_i)_{\overline{\Pi}_{opt}} = 0$, and $\overline{\Pi}_{opt}$ keeps a constant.

Figure 3 shows the characteristic of $\overline{\Pi}_{opt}$ versus corresponding exergy efficiency ($(\eta_{ex})_{\overline{\Pi}_{opt}}$) with $\tau_1 = 5$. It can be seen that the characteristic of $\overline{\Pi}_{opt}$ versus $(\eta_{ex})_{\overline{\Pi}_{opt}}$ is loop-shaped, there exists a maximum dimensionless profit rate ($\overline{\Pi}_{\max}$) and the corresponding exergy efficiency ($(\eta_{ex})_{\overline{\Pi}_{\max}}$). The broken line in the curve exists in the case of $\pi_1 < 1$.

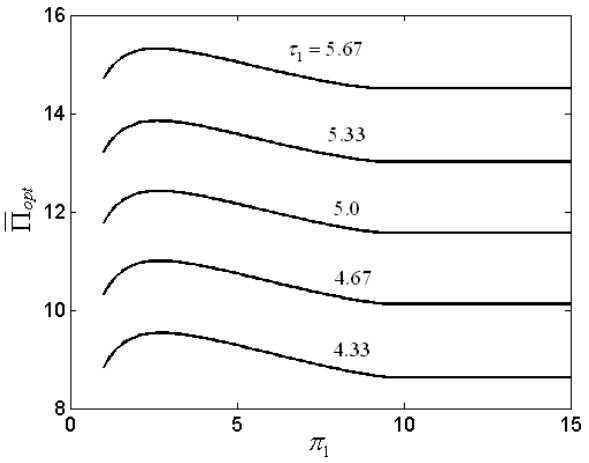

Figure 2. Effect of τ_1 on the characteristic of $\overline{\Pi}_{opt}$ versus π_1

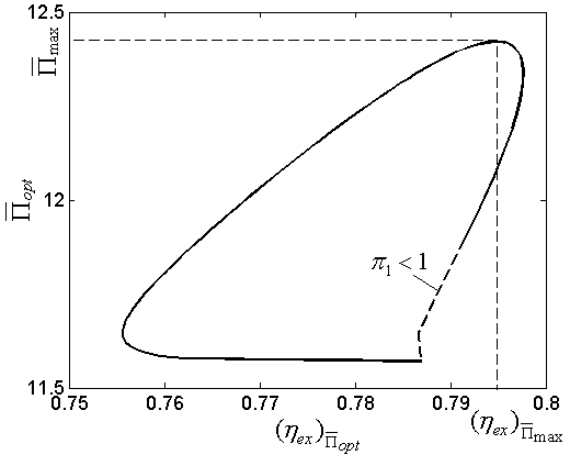

Figure 3. The characteristic of $\overline{\Pi}_{opt}$ versus $(\eta_{ex})_{\overline{\Pi}_{opt}}$

4.2 The maximum dimensionless profit rate

Figure 4 shows the characteristic of the maximum dimensionless profit rate ($\overline{\Pi}_{\max}$) versus π for different τ_1. Figures 5-9 show the characteristics of the corresponding optimal heat conductance allocations ($(u_h)_{\overline{\Pi}_{\max}}$, $(u_l)_{\overline{\Pi}_{\max}}$, $(u_k)_{\overline{\Pi}_{\max}}$, $(u_i)_{\overline{\Pi}_{\max}}$) and optimal intercooling pressure ratio ($(\pi_1)_{\overline{\Pi}_{\max}}$) versus π for different τ_1, respectively. Figure 10 shows the characteristic of $\overline{\Pi}_{\max}$ versus the corresponding exergy efficiency ($(\eta_{ex})_{\overline{\Pi}_{\max}}$) with $\tau_1 = 5$.

It can be seen from Figure 4 that there exists an optimal total pressure ratio ($\pi_{\overline{\Pi}_{\max,2}}$) which make $\overline{\Pi}_{\max}$ reach a double-maximum dimensionless profit rate ($\overline{\Pi}_{\max,2}$) (the corresponding intercooling pressure

ratio is $(\pi_1)_{\overline{\Pi}_{\max,2}}$). $\overline{\Pi}_{\max,2}$ increases with the increase of τ_1. It can be seen from Figures 5-9 that with the increase of π, $(u_h)_{\overline{\Pi}_{\max}}$ and $(u_k)_{\overline{\Pi}_{\max}}$ decrease, $(u_l)_{\overline{\Pi}_{\max}}$, $(u_i)_{\overline{\Pi}_{\max}}$ and $(\pi_1)_{\overline{\Pi}_{\max}}$ increase. With the increase of τ_1, $(u_h)_{\overline{\Pi}_{\max}}$ and $(u_k)_{\overline{\Pi}_{\max}}$ increase, $(u_l)_{\overline{\Pi}_{\max}}$ and $(u_i)_{\overline{\Pi}_{\max}}$ decrease, and $(\pi_1)_{\overline{\Pi}_{\max}}$ decreases slightly. However, when $\pi > 5$, the value of $(u_h)_{\overline{\Pi}_{\max}}$ is about $0.4 \sim 0.5$, the value of $(u_l)_{\overline{\Pi}_{\max}}$ is about 0.1, the value of $(u_k)_{\overline{\Pi}_{\max}}$ is about 0.2, the value of $(u_i)_{\overline{\Pi}_{\max}}$ is about $0.1 \sim 0.2$. It can be seen from Figure 10 that the characteristic of $\overline{\Pi}_{\max}$ versus $(\eta_{ex})_{\overline{\Pi}_{\max}}$ is loop-shaped, there exists a double-maximum dimensionless profit rate ($\overline{\Pi}_{\max,2}$) and the corresponding exergy efficiency ($(\eta_{ex})_{\overline{\Pi}_{\max,2}}$).

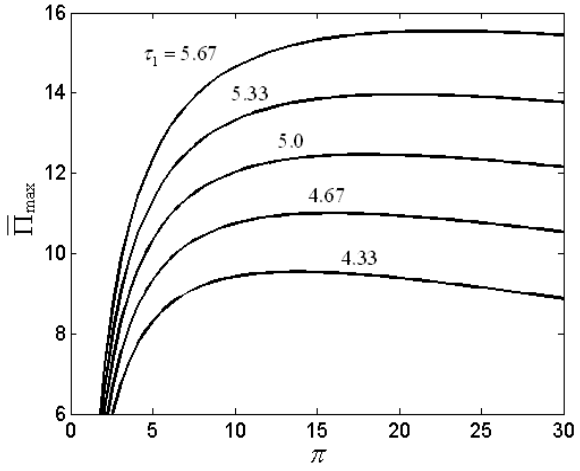

Figure 4. Effect of τ_1 on the characteristic of $\overline{\Pi}_{\max}$ versus π

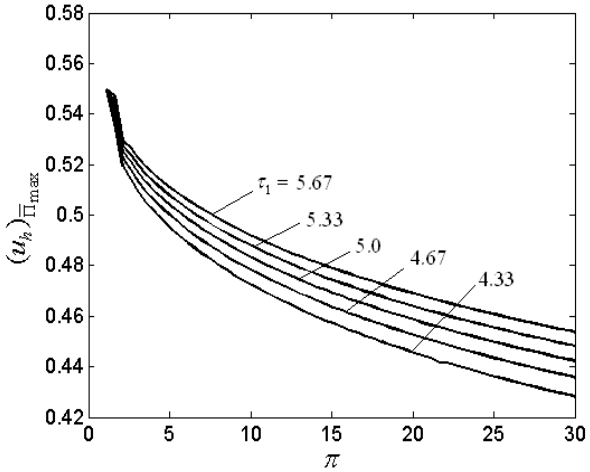

Figure 5. Effect of τ_1 on the characteristic of $(u_h)_{\overline{\Pi}_{\max}}$ versus π

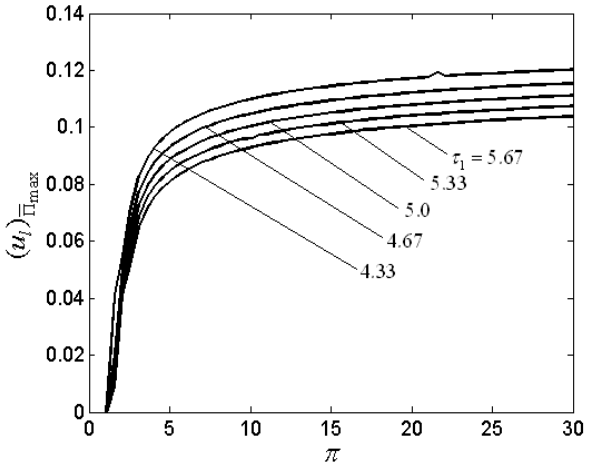

Figure 6. Effect of τ_1 on the characteristic of $(u_l)_{\overline{\Pi}_{\max}}$ versus π

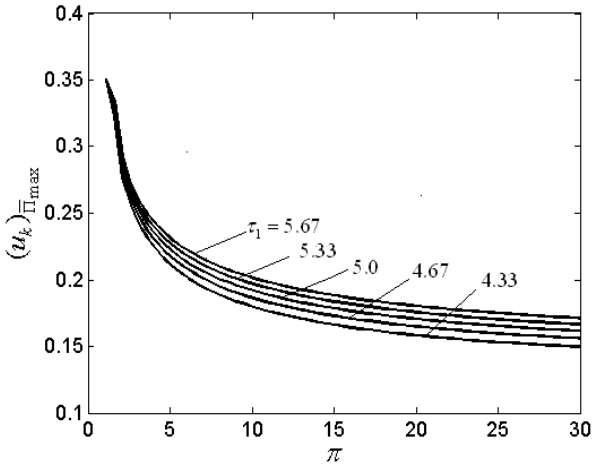

Figure 7. Effect of τ_1 on the characteristic of $(u_k)_{\overline{\Pi}_{\max}}$ versus π

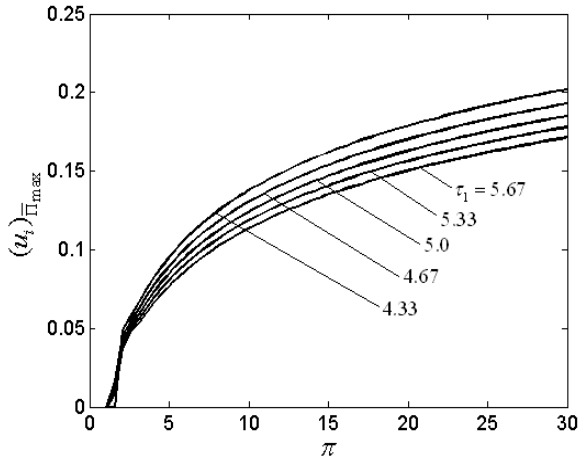

Figure 8. Effect of τ_1 on the characteristic of $(u_i)_{\overline{\Pi}_{max}}$ versus π

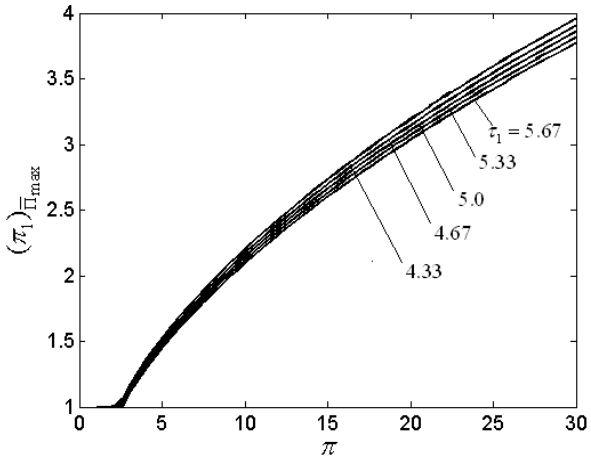

Figure 9. Effect of τ_1 on the characteristic of $(\pi_1)_{\overline{\Pi}_{max}}$ versus π

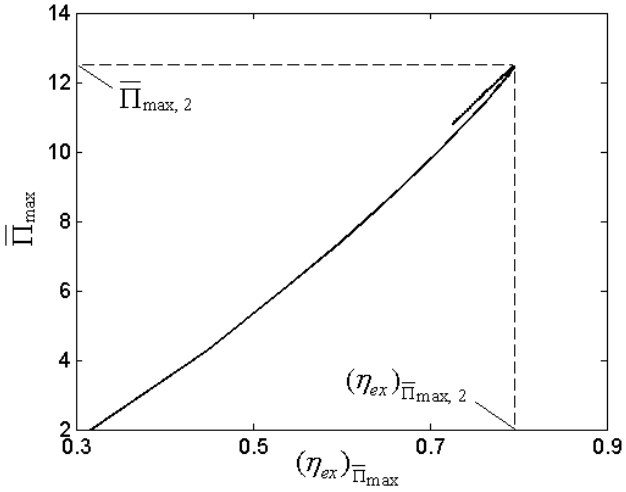

Figure 10. The characteristic of $\overline{\Pi}_{max}$ versus $(\eta_{ex})_{\overline{\Pi}_{max}}$

4.3 The effects of design parameters on the optimal performance

Figures 11-18 show the characteristics of $\overline{\Pi}_{max,\,2}$, $(\eta_{ex})_{\overline{\Pi}_{max,\,2}}$, $(\pi_1)_{\overline{\Pi}_{max,\,2}}$ and $\pi_{\overline{\Pi}_{max,\,2}}$ versus a, b, U_T and τ_4 with $\tau_1 = 5$, respectively. It can be seen from Figures 11-14 that $\overline{\Pi}_{max,\,2}$ increases with the increases of a, b and U_T. When U_T is large, $\overline{\Pi}_{max,\,2}$ increases slowly, there exists an optimal consumer-side temperature ($(\tau_4)_{opt}$) which leads to a thrice-maximum dimensionless profit rate ($\overline{\Pi}_{max,\,3}$). The characteristics of $(\eta_{ex})_{\overline{\Pi}_{max,\,2}}$ versus a, b and τ_4 are parabolic-like, but the value of $(\eta_{ex})_{\overline{\Pi}_{max,\,2}}$ changes slightly with the changes of a and b. The characteristic of $(\eta_{ex})_{\overline{\Pi}_{max,\,2}}$ versus U_T is similar to that of $\overline{\Pi}_{max,\,2}$ versus U_T. It can be seen from Figures 15-18 that $(\pi_1)_{\overline{\Pi}_{max,\,2}}$ increases with the increases of a and U_T. When a is large, $(\pi_1)_{\overline{\Pi}_{max,\,2}}$ increases slowly, $(\pi_1)_{\overline{\Pi}_{max,\,2}}$ decreases with the increase of b. The characteristic of $(\pi_1)_{\overline{\Pi}_{max,\,2}}$ versus τ_4 is parabolic-like. The characteristics of $\pi_{\overline{\Pi}_{max,\,2}}$ versus a, b, U_T and τ_4 are similar to those of $(\pi_1)_{\overline{\Pi}_{max,\,2}}$ versus a, b, U_T and τ_4, respectively.

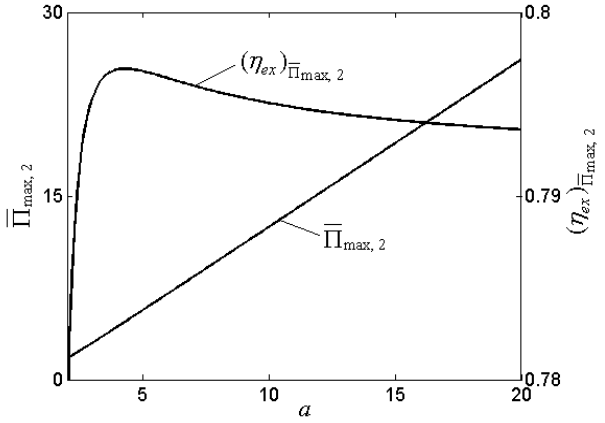

Figure 11. The characteristics of $\overline{\Pi}_{\max,2}$ and $(\eta_{ex})_{\overline{\Pi}_{\max,2}}$ versus a

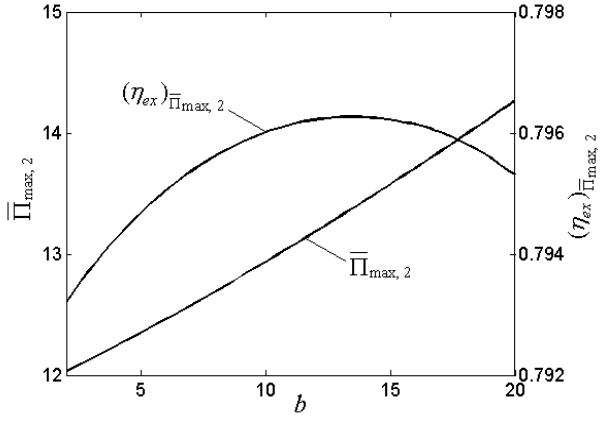

Figure 12. The characteristics of $\overline{\Pi}_{\max,2}$ and $(\eta_{ex})_{\overline{\Pi}_{\max,2}}$ versus b

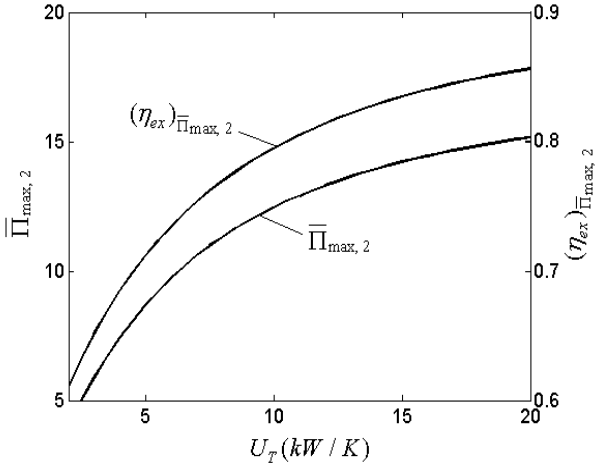

Figure 13. The characteristics of $\overline{\Pi}_{\max,2}$ and $(\eta_{ex})_{\overline{\Pi}_{\max,2}}$ versus U_T

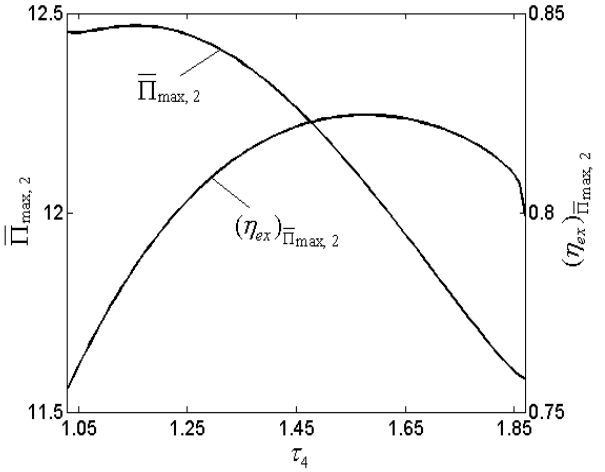

Figure 14. The characteristics of $\overline{\Pi}_{\max,2}$ and $(\eta_{ex})_{\overline{\Pi}_{\max,2}}$ versus τ_4

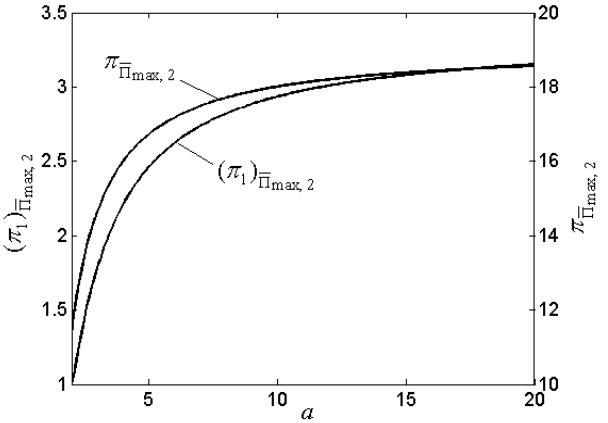

Figure 15. The characteristics of $(\pi_1)_{\overline{\Pi}_{\max,2}}$ and $\pi_{\overline{\Pi}_{\max,2}}$ versus a

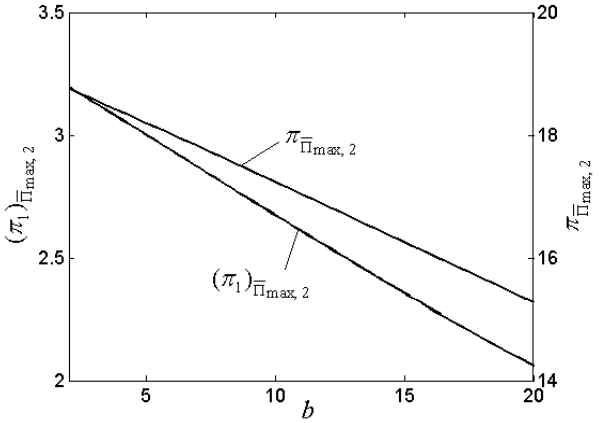

Figure 16. The characteristics of $(\pi_1)_{\overline{\Pi}_{\max,2}}$ and $\pi_{\overline{\Pi}_{\max,2}}$ versus b

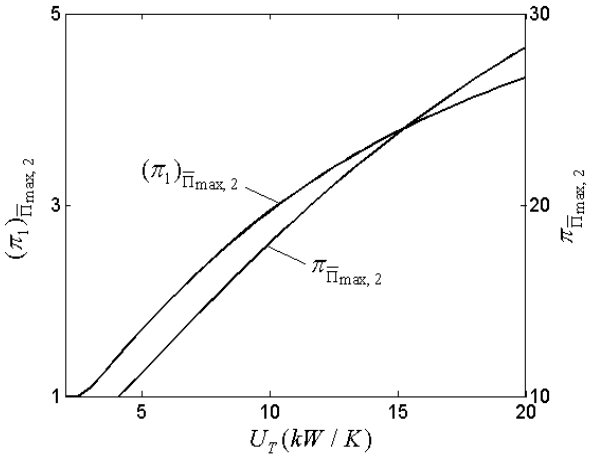

Figure 17. The characteristics of $(\pi_1)_{\overline{\Pi}_{max,2}}$ and $\pi_{\overline{\Pi}_{max,2}}$ versus U_T

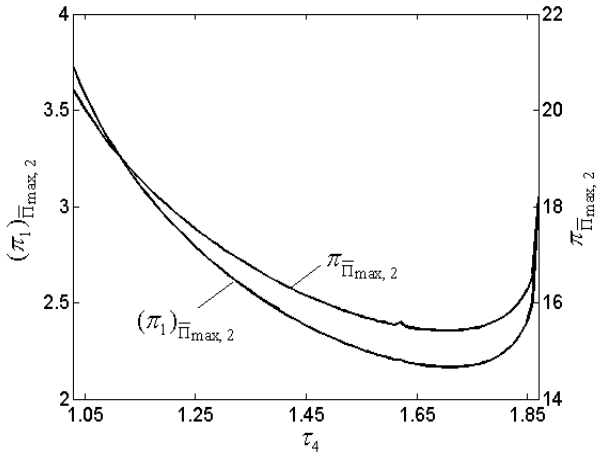

Figure 18. The characteristics of $(\pi_1)_{\overline{\Pi}_{max,2}}$ and $\pi_{\overline{\Pi}_{max,2}}$ versus τ_4

5. Thermal capacity rate matching between the working fluid and heat reservoirs

For the variable-temperature heat reservoirs, the thermal capacity rates of working fluid and heat reservoirs have important influence on the performances of intercooled regenerative Brayton power cycles [47, 48]. Figures 19 and 20 shows the characteristic of $\overline{\Pi}_{max,2}$ versus the thermal capacity rate matching (C_{wf}/C_L) between the working fluid and the cold-side heat reservoir for different C_H/C_L and U_T with $a=10$, $b=6$, $\tau_1=5.0$, $\tau_4=1.2$ and $C_L=C_I=1.2kW/K$. It can be seen that there exists an optimal the thermal capacity rate matching ($(C_{wf}/C_L)_{opt}$) that make $\overline{\Pi}_{max,2}$ reach a thrice-maximum dimensionless profit rate ($\overline{\Pi}_{max,3}$). When $(C_{wf}/C_L)>(C_{wf}/C_L)_{opt}$, $\overline{\Pi}_{max,2}$ decreases rapidly. When $(C_H/C_L)>1$, the effect of C_H/C_L on the characteristic of $\overline{\Pi}_{max,2}$ versus C_{wf}/C_L is slight. When $(C_H/C_L)<1$, with the increase of C_H/C_L, $(C_{wf}/C_L)_{opt}$ increases, and $\overline{\Pi}_{max,3}$ decreases slightly. With the increase of U_T, $(C_{wf}/C_L)_{opt}$ increases, $\overline{\Pi}_{max,3}$ increases slightly.

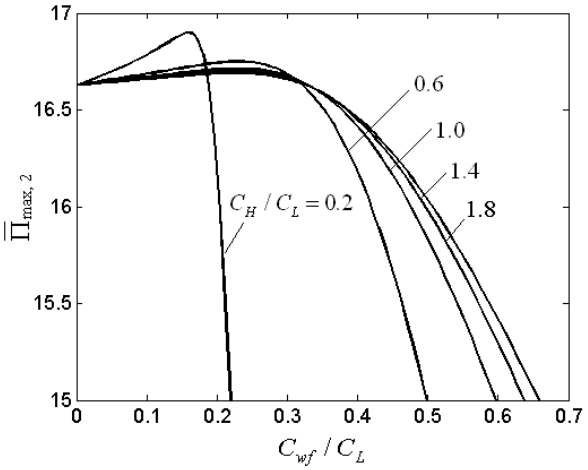

Figure 19. The characteristic of $\overline{\Pi}_{max,2}$ versus C_{wf}/C_L for different C_H/C_L

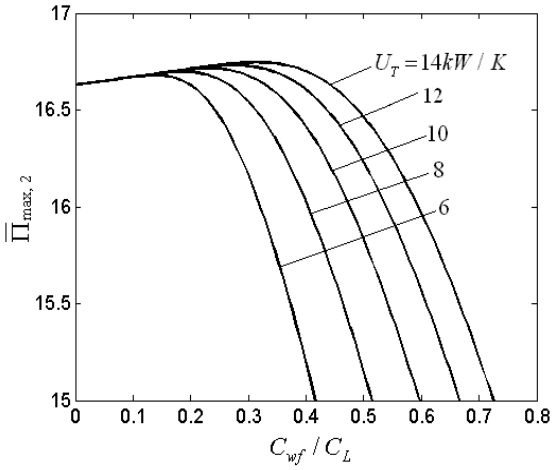

Figure 20. The characteristic of $\overline{\Pi}_{max,2}$ versus C_{wf}/C_L for different U_T

6. Conclusion

Finite time exergoeconomic analyses is applied to perform the profit rate optimization of the CHP plant composed of an endoreversible intercooled regenerative Brayton closed-cycle coupled to variable-temperature heat reservoirs. The results show that the optimal heat conductance allocation of the regenerator is always zero at the design point of the optimal dimensionless profit rate. When the total pressure ratio, the heat conductance allocation of the regenerator and the total heat conductance are fixed, there exists a sole group of optimal heat conductance allocations among the hot-, cold- and consumer-side heat exchangers and the intercooler, and an optimal intercooling pressure ratio which lead to the maximum dimensionless profit rate. When the total pressure ratio is changeable, there exists an optimal total pressure ratio and an optimal intercooling pressure ratio which lead to a double-maximum dimensionless profit rate, and one can obtain that the value of $(u_h)_{\bar{\Pi}_{\max}}$ is about $0.4 \sim 0.5$, the value of $(u_l)_{\bar{\Pi}_{\max}}$ is about 0.1, the value of $(u_k)_{\bar{\Pi}_{\max}}$ is about 0.2, and the value of $(u_i)_{\bar{\Pi}_{\max}}$ is about $0.1 \sim 0.2$, respectively. The characteristic of the maximum dimensionless profit rate versus the corresponding exergy efficiency is studied and the characteristic is loop-shaped. The effects of some design parameters on the double-maximum dimensionless profit rate and the corresponding exergy efficiency, optimal total pressure ratio and optimal intercooling pressure ratio are discussed in detail. It is found that there exists an optimal consumer-side temperature which lead to a thrice-maximum dimensionless profit rate. When the optimization is performed additionally with respect to the thermal capacitance rate matching between the working fluid and the heat reservoirs, a thrice-maximum profit rate is obtained.

Acknowledgements

This paper is supported by The National Natural Science Foundation of P. R. China (Project No. 10905093), The Program for New Century Excellent Talents in University of P. R. China (Project No. NCET-04-1006) and The Foundation for the Author of National Excellent Doctoral Dissertation of P. R. China (Project No. 200136).

Nomenclature

a	price ratio of power output to exergy input rate
b	price ratio of thermal exergy output rate to exergy input rate
C	heat capacity rate (kW / K)
E	effectiveness of the heat exchanger
e	exergy flow rate (kW)
k	ratio of the specific heats
N	number of heat transfer units
P	power output of the cycle (kW)
Q	rate of heat transfer (kW)
s	entropy (kJ / K)
T	temperature (K)
U	heat conductance (kW / K)
u_h	hot-side heat conductance allocation
u_i	heat conductance allocation of the intercooler
u_k	consumer-side heat conductance allocation
u_l	cold-side heat conductance allocation
u_r	heat conductance allocation of the regenerator
x	isentropic temperature ratio for low-pressure compressor
y	isentropic temperature ratio for total compression process

Greek symbols

φ	price of exergy flow rate ($dollar / kW$)
η	efficiency
Π	profit rate ($dollar$)
π_1	intercooling pressure ratio
π	total pressure ratio
σ	entropy generation rate of the cycle (kW / K)

τ_1	ratio of the inlet temperature of hot-side heat reservoir to environment temperature
τ_2	ratio of the inlet temperature of cold-side heat reservoir to environment temperature
τ_3	ratio of the inlet temperature of intercooling fluid to environment temperature
τ_4	ratio of the consumer-side temperature to environment temperature

Subscripts

ex	exergy
H	hot-side
I	intercooler
in	inlet
K	consumer-side
L	cold-side
max	maximum
min	minimum
opt	optimal
out	outlet
R	regenerator
T	total
wf	working fluid
0	ambient
$1,2,3,4,5,6,7,8,9$	state points of the cycle
$^-$	dimensionless

References

[1] Habib M A. Thermodynamic analysis of the performance of cogeneration plants. Energy, The Int. J., 1992, 17(5): 485-491.

[2] Rosen M A, Le M N, Dincer I. Exergetic analysis of cogeneration-based district energy systems. Proc. IMechE, Part A: J. Power Energy, 2004, 218(6): 369-375.

[3] Khaliq A. Exergy analysis of gas turbine trigeneration system for combined production of power heat and refrigeration. Int. J. Refrig., 2009, 32(3): 534-545.

[4] Reddy B V, Butcher C. Second law analysis of a natural gas-fired gas turbine cogeneration system. Int. J. Energy Res., 2009, 39(8): 728-736.

[5] Khaliq A, Choudhary K. Thermodynamic evaluation of gas turbines for cogeneration applications. Int. J. Exergy, 2009, 6 (1): 15-33.

[6] Andresen B. Finite Time Thermodynamics. Physics Laboratory II, University of Copenhagen, 1983.

[7] Bejan A. Entropy generation minimization: The new thermodynamics of finite-size devices and finite-time process. J. Appl. Phys., 1996, 79(3): 1191-1218.

[8] Berry R S, Kazakov V A, Sieniutycz S, Szwast Z, Tsirlin A M. Thermodynamic Optimization of Finite Time Processes. Chichester: Wiley, 1999.

[9] Chen L, Wu C, Sun F. Finite time thermodynamic optimization of entropy generation minimization of energy systems. J. Non-Equilibrium Thermodyn., 1999, 24(4): 327-359.

[10] Durmayaz A, Sogut O S, Sahin B and Yavuz H. Optimization of thermal systems based on finite-time thermodynamics and thermoeconomics. Progr. Energy Combus. Sci., 2004, 30(2): 175-217.

[11] Chen L, Sun F. Advances in Finite Time Thermodynamics: Analysis and Optimization. New York: Nova Science Publishers, 2004.

[12] Ust Y, Sahin B, Safa A. Ecological performance analysis of an endoreversible regenerative Brayton heat-engine. Appl. Energy, 2005, 80(3): 247-260.

[13] Ust Y, Sahin B, Kodal A. Performance analysis of an irreversible Brayton heat engine based on ecological coefficient of performance criterion. Int. J. Thermal Sci., 2006, 45(1): 94-101.

[14] Ust Y, Sogut O S, Sahin B, Durmayaz A. Ecological coefficient of performance (ECOP) optimization for an irreversible Brayton heat engine with variable-temperature thermal reservoirs. J. Energy Instit., 2006, 79(1): 47-52.

[15] Ust Y, Sahin B, Kodal A, Akcay I H. Ecological coefficient of performance analysis and optimization of an irreversible regenerative Brayton heat engine. Appl. Energy, 2006, 83(6): 558-572.
[16] De Vos A. Thermodynamics of Solar Energy Conversion. Berlin: Wiley-Vch, 2008.
[17] Feidt M. Optimal thermodynamics-New upperbounds. Entropy, 2009, 11(4): 529-547.
[18] Sieniutycz S, Jezowski J. Energy Optimization in Process Systems. Elsevier, Oxford, UK, 2009.
[19] Bojic M. Cogeneration of power and heat by using endoreversible Carnot engine. Energy Convers. Mgmt., 1997, 38(18): 1877-1880.
[20] Sahin B, Kodal A, Ekmekci I, Yilmaz T. Exergy optimization for an endoreversible cogeneration cycle. Energy, The Int. J., 1997, 22(5): 551-557.
[21] Erdil A. Exergy optimization for an irreversible combined cogeneration cycle. J. Energy Instit., 2005, 75(1): 27-31.
[22] Atmaca M, Gumus M, Inan A T, Yilmaz T. Optimization of irreversible cogeneration systems under alternative performance criteria. Int. J. Thermophys., 2009, 30(5): 1724-1732.
[23] Ust Y, Sahin B, Kodal A. Performance optimisation of irreversible cogeneration systems based on a new exergetic performance criterion: exergy density. J. Energy Instit., 2009, 82(1): 48-52.
[24] Yilmaz T. Performance optimization of a gas turbine-based cogeneration system. J. Phys. D: Appl. Phys., 2006, 39(11): 2454-2458.
[25] Hao X, Zhang G. Maximum useful energy-rate analysis of an endoreversible Joule-Brayton cogeneration cycle. Appl. Energy, 2007, 84(11): 1092-1101.
[26] Hao X, Zhang G. Exergy optimisation of a Brayton cycle-based cogeneration plant. Int. J. Exergy, 2009, 6(1): 34-48.
[27] Ust Y, Sahin B, Yilmaz T. Optimization of a regenerative gas-turbine cogeneration system based on a new exergetic performance criterion: exergetic performance coefficient. Proc. ImechE, Part A: J. Power Energy, 2007, 221(4): 447-458.
[28] Ust Y, Sahin B, Kodal A. Optimization of a dual cycle cogeneration system based on a new exergetic performance criterion. Appl. Energy, 2007, 84(11): 1079 -1091.
[29] Tsatsaronts G. Thermoeconomic analysis and optimization of energy systems. Progr. Energy Combus. Sci., 1993, 19(3): 227-257.
[30] El-Sayed M. Thermoeconomics of Energy Conversion. London: Elsevier, 2003.
[31] Salamon P, Nitzan A. Finite time optimizations of a Newton's law Carnot cycle. J. Chem. Phys., 1981, 74(6): 3546-3560.
[32] Chen L, Sun F, Chen W. The relation between optimal efficiency and profit rate of a Cannot engine. J. Engng. Thermal Energy Power, 1991, 6(4): 237-240 (in Chinese).
[33] Sun F, Chen L, Chen W. The efficiency and profit holographic spectrum of a two-heat-reservoir heat engine. Trans. Chin. Soc. Internal Combus. Engines, 1991, 9(3): 286-287 (in Chinese).
[34] Chen L, Sun F, Wu C. Exergoeconomic performance bound and optimization criteria for heat engines. Int. J. Ambient Energy, 1997, 18(4): 216-218.
[35] Wu C, Chen L, Sun F. Effect of heat transfer law on finite time exergoeconomic performance of heat engines. Energy, The Int. J., 1996, 21(12): 1127-1134.
[36] Chen L, Sun F, Chen W. Finite time exergoeconomic performance bound and optimization criteria for two-heat-reservoir refrigerators. Chin. Sci. Bull., 1991, 36(2): 156-157 (in Chinese).
[37] Chen L, Wu C, Sun F. Effect of heat transfer law on finite time exergoeconomic performance of a Carnot refrigerator. Exergy, An Int. J., 2001, 1(4): 295-302.
[38] Wu C, Chen L, Sun F. Effect of heat transfer law on finite time exergoeconomic performance of a Carnot heat pump. Energy Convers. Mgnt., 1998, 39(7): 579-588.
[39] Zheng Z, Chen L, Sun F, Wu C. Maximum profit performance for a class of universal steady flow endoreversible heat engine cycles. Int. J. Ambient Energy, 2006, 27(1): 29-36.
[40] Chen L, Sun F, Wu C. Maximum profit performance for generalized irreversible Carnot engines. Appl. Energy, 2004, 79(1): 15-25.
[41] Chen L, Zheng Z, Sun F, Wu C. Profit performance optimisation for an irreversible Carnot refrigeration cycle. Int. J. Ambient Energy, 2008, 29(4): 197-206.
[42] Tao G, Chen L, Sun F, Wu C. Exergoeconomic performance optimization for an endoreversible simple gas turbine closed-cycle cogeneration plant. Int. J. Ambient Energy, 2009, 30(3): 115-124.

[43] Tao G, Chen L, Sun F. Exergoeconomic performance optimization for an endoreversible regenerative gas turbine closed-cycle cogeneration plant. Riv. Mex. Fis., 2009, 55(3): 192-200.
[44] Chen L, Yang B, Sun F. Exergoeconomic performance optimization of an endoreversible intercooled regenerated Brayton cogeneration plant. Part 1: thermodynamic model and parameter analyses. Int. J. Energy and Environment, 2011, 2(2): 199-210.
[45] Yang B, Chen L, Sun F. Exergoeconomic performance optimization of an endoreversible intercooled regenerated Brayton cogeneration plant. Part 2: heat conductance allocation and pressure ratio optimization. Int. J. Energy and Environment, 2011, 2(2): 211-218.
[46] Yang B, Chen L, Sun F. Exergoeconomic performance analyses of an endoreversible intercooled regenerative Brayton cogeneration type model. Int. J. Sustainable Energy, 2011, 30(2): 65-81.
[47] Wang W, Chen L, Sun F, Wu C. Power optimization of an endoreversible closed intercooled regenerated Brayton cycle coupled to variable-temperature heat reservoirs. Appl. Energy, 2005, 82(2): 181-195.
[48] Wang W, Chen L, Sun F, Wu C. Efficiency optimization of an irreversible closed intercooled regenerated gas-turbine cycle. Proc. IMechE, Part A: J. Power Energy, 2006, 220(A6): 551-558.
[49] Chen L, Wang J, Sun F. Power density optimisation of an endoreversible closed intercooled regenerated Brayton cycle. J. Energy Instit., 2007, 80(2): 105-109.
[50] Fang G, Cai R, Lin R. Analysis on basic parameters in cogeneration cycle with gas turbine and steam turbine. J. Power Engng., 1998, 8(6): 118-124 (in Chinese).

Bo Yang received his BS Degree in 2008 and MS Degree in 2010 in power engineering and engineering thermophysics from the Naval University of Engineering, P R China. He is pursuing for his PhD Degree in power engineering and engineering thermophysics of Naval University of Engineering, P R China. His work covers topics in finite time thermodynamics and technology support for propulsion plants. Dr Yang is the author or co-author of 11 peer-refereed articles (5 in English journals).

Lingen Chen received all his degrees (BS, 1983; MS, 1986, PhD, 1998) in power engineering and engineering thermophysics from the Naval University of Engineering, P R China. His work covers a diversity of topics in engineering thermodynamics, constructal theory, turbomachinery, reliability engineering, and technology support for propulsion plants. He has been the Director of the Department of Nuclear Energy Science and Engineering, the Director of the Department of Power Engineering and the Superintendent of the Postgraduate School. Now, he is the Dean of the College of Naval Architecture and Power, Naval University of Engineering, P R China. Professor Chen is the author or co-author of over 1200 peer-refereed articles (over 520 in English journals) and nine books (two in English).
E-mail address: lgchenna@yahoo.com; lingenchen@hotmail.com, Fax: 0086-27-83638709 Tel: 0086-27-83615046

Fengrui Sun received his BS degree in 1958 in Power Engineering from the Harbing University of Technology, P R China. His work covers a diversity of topics in engineering thermodynamics, constructal theory, reliability engineering, and marine nuclear reactor engineering. He is a Professor in the Department of Power Engineering, Naval University of Engineering, P R China. Professor Sun is the author or co-author of over 750 peer-refereed papers (over 340 in English) and two books (one in English).

